

NASA TM X-56019

PERFORMANCE OF A BALLUTE DECELERATOR  
TOWED BEHIND A JET AIRPLANE

Jon S. Pyle, James R. Phelps, and Robert S. Baron

December 1973

NASA Flight Research Center  
Edwards, California 93523

# PERFORMANCE OF A BALLUTE DECELERATOR TOWED BEHIND A JET AIRPLANE

Jon S. Pyle, James R. Phelps, and Robert S. Baron  
Flight Research Center

## SUMMARY

An F-104B airplane was modified to investigate the drag and stability characteristics of a ballute decelerator in the wake of an asymmetrical airplane. Decelerator deployments were initiated at a Mach number of 1.3 and an altitude of 15,240 meters (50,000 feet) and terminated when the airplane had decelerated to a Mach number of 0.5. The flight tests indicated that the decelerator had a short inflation time with relatively small opening forces. The drag levels attained with the subject decelerator were less than those obtained with other high-speed decelerators behind a symmetrical tow vehicle. The ballute demonstrated good stability characteristics behind the testbed airplane.

## INTRODUCTION

The development of aerodynamic decelerators capable of withstanding the compressible-flow environment has been one of the primary research objectives in the field of parachute technology for the past decade. Although parachutes of the canopy type are reliable devices for aircraft stabilization and recovery at subsonic speeds, they are not suitable for the complex shock patterns and flow fields in the wake of vehicles traveling at transonic to hypersonic speeds.

Many types of decelerators have been tested in wind-tunnel facilities (refs. 1 to 10) in an effort to develop a configuration that will satisfy the requirements of the transonic, supersonic, and hypersonic flight environments. One of these evolved into a configuration called the ballute decelerator, which is a ram-inflated cone sphere developed by Goodyear Aerospace Corporation (refs. 11 and 12). This configuration has shown good stability and high drag characteristics through a wide Mach number range behind a variety of symmetrically shaped vehicles (refs. 13 to 17). Few flight results have been obtained with this configuration behind an asymmetrical vehicle, however.

There was considerable uncertainty about the stability of lifting body vehicles in the transonic Mach number region before they were tested in flight. Also, at that time, high-speed airplanes could not rely on drag parachutes for emergency stabilization at transonic and supersonic Mach numbers. Therefore, consideration was given to flight

testing a stabilization-deceleration device that could be deployed in the high-speed portion of these vehicles' flight envelopes. The device had to be light in weight and small in volume. The success of the ballute decelerator in earlier SV-5 PRIME (Precision Recovery Including Maneuvering Entry) lifting body flight tests conducted by the Air Force (ref. 18) and its immediate availability prompted the selection of this device for the present program.

Modifications were made to an F-104B airplane so that a ballute decelerator could be flight tested in its asymmetrical wake. The flight tests were performed at Mach numbers from 1.3 to 0.5 and dynamic pressures between 9.6 and 16.8 kilonewtons per square meter (200 to 350 pounds per square foot). This paper describes the operational problems that were encountered during the flight tests, and presents data for the inflation time and drag coefficient of the decelerator system. The decelerator's stability in the aircraft wake is illustrated by sketches from high-speed moving pictures. The drag forces measured in flight behind the asymmetrical vehicle are compared with similar flight and wind-tunnel results obtained behind symmetrical vehicles.

## SYMBOLS

Physical quantities in this report are given in the International System of Units (SI) and parenthetically in U.S. Customary Units. Measurements were taken in U.S. Customary Units. Details concerning the use of SI, together with physical quantities and conversion factors, are given in reference 19.

$C_{DA}$	drag coefficient based on the maximum cross-sectional area of the decelerator
d	diameter of the decelerator, m (ft)
h	altitude, m (ft)
l	length of towline behind the jet engine exhaust exit, m (ft)
M	free-stream Mach number
q	free-stream dynamic pressure, $\text{kN/m}^2$ ( $\text{lb/ft}^2$ )
t	time after mortar ignition, sec

## TEST CONFIGURATION

### Test Vehicle

An F-104B airplane (fig. 1) was used as the test bed for the decelerator tests. The basic vehicle was equipped with a drag chute compartment on the bottom of the fuselage 1.93 meters (6.3 feet) in front of the jet engine exhaust. This compartment was replaced by a specially designed decelerator compartment (fig. 2). The SV-5 PRIME decelerator

package was mounted in the new compartment along with a low-speed (24-frame-per-second) camera and a high-speed (220-frame-per-second) camera. The attachment linkage necessary to connect the decelerator to an existing mechanical release hook on the aircraft was installed. Multiple release mechanisms were designed into the attachment linkage to improve the operational safety of the testbed vehicle. The attachment linkage is discussed in the section entitled "Operational History."

### Ballute Decelerator

The ballute decelerator is a ram-air-inflated,  $80^\circ$  cone sphere with a 10-percent-diameter burble fence located at its maximum diameter (fig. 1). The ballute is ram air inflated by means of four inlets located symmetrically around the decelerator. The ballutes used in these tests were of nylon material with an elastic coating that reduced porosity. A 9.1-meter (30-foot) nylon riser line extended from the apex of the ballute to the attachment linkage in the drag chute compartment of the F-104B airplane. This line length was necessary to obtain line-length-to-diameter ratios compatible with wind-tunnel and additional flight tests with the ballute (refs. 14 and 17). The maximum diameter of the ballute, fully inflated, was 1.22 meters (4.0 feet). The decelerator is described in more detail in reference 12.

### Decelerator Deployment

The decelerator package, which contained the ballute and the nylon riser line, was obtained from the SV-5 PRIME project and was adapted to the modified drag chute compartment of the F-104B airplane. The dimensions of the decelerator package and its contents are shown in figure 3. The decelerator was deployed by firing a mortar charge at the base of the package. The explosive charge forced the sabot (a plastic piston device in the deployment bag) forward, broke the rivets on the package door, and pushed the deployment bag into the wake of the airplane. A side view of the rear of the airplane showing the decelerator deployment bag just after firing the mortar is shown in figure 4(a) along with a sketch of a photograph taken at the same point in the deployment sequence. When the deployment bag reached the end of the external nylon riser line (fig. 4(b)), the cords on the bag were severed and the deployment bag was pulled from the decelerator (fig. 4(c)). The decelerator began to inflate (fig. 4(d)) by means of four spring-loaded ram-air inlets located just in front of the burble fence. The decelerator was usually inflated completely approximately 1 second after firing (fig. 4(e)).

### Instrumentation and Accuracy

An onboard portable instrumentation package and a magnetic tape recording system were used to sense and record pertinent decelerator and aircraft parameters.

The onboard instrumentation included a standard NACA pitot-static probe and vane sensors mounted on the nose of the test airplane to determine airspeed, altitude, angle of attack, and angle of sideslip (ref. 20).

Airspeed and altitude measurements were corrected for position errors and are accurate to  $\pm 6$  percent and  $\pm 7$  percent, respectively. The angle-of-attack and -sideslip

measurements were observed for attitude reference purposes, but were not used to determine the load factor or drag coefficient of the decelerator.

The drag force imposed upon the airplane by the decelerator was determined by a drag link in the linkage assembly (fig. 2(a)). The drag link was instrumented with two strain gage bridges; both outputs were recorded on the onboard magnetic tape. Each bridge consisted of two active gages oriented so that they measured axial loads and two compensating gages. Each gage was of the phenolic-glass constantan-foil type with a gage factor of 2.13, had a resistance of 350 ohms, and was temperature compensated for 6 parts per million.

The drag link was calibrated by applying tension loads from 0 to 3400 kilograms (0 to 7500 pounds). After cycling the gages several times and balancing the bridges, the link was calibrated with tension loads that were varied in 227 ( $\pm 16$ )-kilogram (500 ( $\pm 35$ )-pound) increments from minimum to maximum to minimum. The maximum deviation due to hysteresis and repeatability for both bridges was  $\pm 23$  kilograms ( $\pm 50$  pounds). The maximum deviation in measured drag force between the two bridges during the flight tests discussed in this paper was  $\pm 55$  kilograms ( $\pm 120$  pounds), which is approximately 5 percent of the measured drag force. The root-sum-square error for the drag force measured during the flight tests of the decelerator was therefore  $\pm 35$  kilograms ( $\pm 80$  pounds), or  $\pm 2.5$  percent of the average measured drag force.

## TEST PROCEDURES

To insure the safety of the airplane-decelerator configuration at high transonic Mach numbers, deployments were performed at progressively increasing vehicle speeds, beginning at a Mach number of 0.5 and increasing to a Mach number of 1.3.

Prior to decelerator deployment, the airplane was flown to a predetermined altitude and velocity along a known flight path with the aid of radar tracking. At the designated point, the decelerator was deployed by the pilot. During deceleration, the pilot tried to maintain a constant dynamic pressure by controlling the airplane's altitude. The tests were terminated when the airplane reached an altitude of 1524 meters (5000 feet), when the pilot released the decelerator and towline and allowed them to fall to the ground to be recovered. Nine flight tests were performed in this manner, with the last two deployments occurring at a Mach number of 1.3 and an altitude of approximately 15,240 meters (50,000 feet).

## OPERATIONAL HISTORY

A series of operational problems caused by the attachment linkage between the decelerator and the airplane occurred during the flight tests. These problems are described below so that they can be avoided in future flight tests.

The attachment linkage consisted of a drag link that was instrumented with strain gages and shaped to fit the mechanical release system of the drag chute in the airplane. The drag link was connected to a swivel harness by means of a bolt machined to break under a tension load of 22.2 kilonewtons (5000 pounds). The bolt was fastened at each

end with explosive nuts that could be ignited individually by the pilot. This provided a double-redundant mechanical and a double-redundant electrical release system for the decelerator. The swivel unit of the linkage was attached directly to the nylon riser line of the decelerator.

Flight tests of this linkage system revealed a gradual deterioration of the nylon riser line due to its rubbing against the sides of the modified drag chute compartment. In addition, the decelerator spun at a very high rate (approaching 500 revolutions per minute) during some of the later flights, inducing high torsion loads in the riser line. Therefore the linkage system was modified as shown in figure 5. The guide bar was attached to the drag link by the machined bolt and the explosive nuts. The swivel was moved behind the guide bar so that it relieved the torsion load caused by the spinning decelerator. The spinning of the ballute was caused by asymmetry in the ram-air inlets and small rips in the decelerator fabric. These problems were corrected, and the spin rates of the decelerator during the subsequent flight tests were much lower.

## TESTS RESULTS

### Inflation Characteristics

The flight results presented in this paper were obtained with the F-104B airplane trailing a ballute decelerator at a Mach number of 1.3 and an altitude of approximately 15,240 meters (50,000 feet). Figure 6 is a time history of the inflation drag force during two deployments. The time histories indicate that the decelerator inflated at a very rapid rate. Although the drag force was somewhat erratic during the inflation period, it was usually less than 60 percent of the peak opening force common to canopy parachutes at lower speeds (ref. 21). The sketches in figures 7(a) to 7(d), which are from photographs taken with the high-speed camera, show a typical decelerator inflation. The sketches are further evidence of the small amount of flexing and the short duration of the inflation process.

### Drag Characteristics

Figures 8(a) and 8(b) are time histories of Mach number, altitude, dynamic pressure, and drag force for the two flight tests discussed. Flight results from both tests are presented to indicate the repeatability of the data. The differences in dynamic pressure between the two decelerations caused the differences in drag force level. The gradients approximately 50 seconds after mortar ignition were due to variation in drag force as the airplane-decelerator system passed back into the incompressible flow region.

The results were nondimensionalized by using the area of the ballute as the reference area so that these flight results could be compared with test results for symmetrical tow vehicles. The variation of drag coefficient with Mach number is presented in figure 9 for the two flights discussed herein, and the agreement between the sets of data is good.

Figure 10 compares the faired flight results of this study with test results for the ballute decelerator towed by symmetrical vehicles. The results from reference 17 were obtained with an inflatable ballute towed behind a symmetrical payload. This

ballute was also 1.2 meters (4 feet) in diameter when inflated. The wind-tunnel results (ref. 14) were obtained with a solid ballute model mounted behind a symmetrical payload.

The ratios of line length to diameter ( $l/d$ ) ranged from 7.5 to 9 for these tests. These line lengths should have placed the decelerator beyond the point (called the critical separation point in reference 14) where the wakes converged behind the symmetrical vehicles. However, the flight tests with the F-104B airplane were terminated before the decelerator could be deployed with various line lengths to determine its critical separation point.

At speeds above a Mach number of 1.0, the drag levels for a ballute in the wake of an asymmetrical tow vehicle are less than they are for one behind a symmetrical tow vehicle. The difference may be due to towing the decelerator in front of the critical separation point for the asymmetrical vehicle. In future tests of ballute decelerators behind asymmetrical vehicles, the critical separation point for each towing body should be determined.

### STABILITY CHARACTERISTICS

It was the general opinion of observers both on the ground and in chase aircraft that the ballute was extremely stable throughout the Mach number range of the flight tests. These observations were substantiated by photographs from the high-speed camera. There was no evidence of coning (circular movement of the ballute with the apex of the cone at the point where the riser line is attached to the swivel or the decelerator is attached to the riser line), or pulsing (breathing), which are commonly exhibited by parachute decelerators at transonic speeds. However, severe spin rates were noted during three flights (see "Operational History"). During the last two flights some spinning (at rates under 100 revolutions per minute) occurred at the higher Mach numbers, but it stopped within 25 seconds after deployment.

The only noticeable decelerator movement during either flight is shown in the sequence of sketches in figure 11. In the 14-second period presented, the decelerator moved upward toward the center of the airplane wake. The last photographs in the series were taken during a turn in which the airplane was flown at high angles of attack and normal accelerations.

### CONCLUDING REMARKS

An F-104B airplane was modified to investigate the drag and stability characteristics of a ballute decelerator in the wake of an asymmetrical airplane. Decelerator deployments were initiated at a Mach number of 1.3 and an altitude of 15,240 meters (50,000 feet) and terminated when the airplane had decelerated to a Mach number of 0.5. The flight tests indicated that the decelerator has a rapid inflation time with relatively small opening forces. The drag levels attained with the subject decelerator were less than those obtained with the other high-speed decelerators behind a symmetrical tow

vehicle. The ballute demonstrated good stability characteristics behind the testbed airplane.

Flight Research Center

National Aeronautics and Space Administration

Edwards, Calif., December 12, 1973



## REFERENCES

1. Engstrom, B. A.; and Meyer, R. A.: Performance of Trailing Aerodynamic Decelerators at High Dynamic Pressures. Part III - Wind Tunnel Testing of Rigid and Flexible Parachute Models. WADC Tech. Rep. 58-284, Wright Air Dev. Div., Wright-Patterson AFB, 1959.
2. McShera, John T.; and Keyes, J. Wayne: Wind-Tunnel Investigation of a Balloon as a Towed Decelerator at Mach Numbers From 1.47 to 2.50. NASA TN D-919, 1961.
3. Charczenko, Nickolai; and McShera, John T.: Aerodynamic Characteristics of Towed Cones Used as Decelerators at Mach Numbers From 1.57 to 4.65. NASA TN D-994, 1961.
4. Berndt, Rudi J.: Supersonic Parachute Research. ASD-TDR-62-236, Aeron. Systems Div., Wright-Patterson AFB, May 1962.
5. McShera, John T., Jr.: Aerodynamic Drag and Stability Characteristics of Towed Inflatable Decelerators at Supersonic Speeds. NASA TN D-1601, 1963.
6. Charczenko, Nickolai: Aerodynamic Characteristics of Towed Spheres, Conical Rings, and Cones Used as Decelerators at Mach Numbers From 1.57 to 4.65. NASA TN D-1789, 1963.
7. Deitering, J. S.: Performance of Flexible Aerodynamic Decelerators at Mach Numbers From 1.5 to 6. AEDC-TDR-63-119, Arnold Engineering Dev. Center, Arnold Air Force Station, July 1963.
8. Charczenko, Nickolai: Wind-Tunnel Investigation of Drag and Stability of Parachutes at Supersonic Speeds. NASA TM X-991, 1964.
9. Galigher, Lawrence L.: Aerodynamic Characteristics of Ballutes and Hemisflo Parachutes at Mach Numbers of 2.5, 2.6, and 2.9. AEDC-TR-65-105, Arnold Engineering Dev. Center, Arnold Air Force Station, May 1965.
10. MacLanahan, D. A., Jr.: An Investigation of Various Types of Decelerators at Mach Number 2.8. AEDC-TR-66-136, Arnold Engineering Dev. Center, Arnold Air Force Station, July 1966.
11. Anon.: PEPP Ballute Design and Development. Final Report. NASA CR-66585, 1967.
12. Anon.: Design of Disk-Gap-Band and Modified Ringsail Parachutes and Development of Ballute Apex Inlet for Supersonic Application. NASA CR-66909, 1970.
13. Nebiker, F. R.: Aerodynamic Deployable Decelerator Performance-Evaluation Program. Tech. Rep. AFFDL-TR-65-27, Air Force Flight Dynamics Lab., Wright-Patterson AFB, Aug. 1965.

14. Turk, Raymond A.: Pressure Measurements on Rigid Model of Ballute Decelerator at Mach Numbers From 0.56 to 1.96. NASA TN D-3545, 1966.
15. McShera, John T., Jr.; and Bohon, Herman L.: A Summary of Supersonic Decelerators With Emphasis on Problem Areas in Aerodynamics and Structures. NASA TM X-59622, 1967.
16. Bloetscher, F.: Aerodynamic Deployable Decelerator Performance-Evaluation Program — Phase II. AFFDL-TR-67-25, Air Force Flight Dynamics Lab., Wright-Patterson AFB, June 1967.
17. Usry, J. W.: Performance of a Towed, 48-Inch-Diameter (121.92-cm) Ballute Decelerator Tested in Free Flight at Mach Numbers From 4.2 to 0.4. NASA TN D-4943, 1969.
18. Sterhardt, J. A., Jr.: SV-5D Project PRIME Lifting Re-Entry Vehicle Development. Proceedings of Asset/Advanced Lifting Re-Entry Technology Symposium, AFFDL-TR-66 22, Air Force Flight Dynamics Lab., Wright-Patterson AFB, Mar. 1966, pp. 1003-1063.
19. Mechtly, E. A.: The International System of Units — Physical Constants and Conversion Factors. Second Revision. NASA SP-7012, 1973.
20. Larson, Terry J.; and Webb, Lannie D.: Calibrations and Comparisons of Pressure-Type Airspeed-Altitude Systems of the X-15 Airplane From Subsonic to High Supersonic Speeds. NASA TN D-1724, 1963.
21. Anon.: Performance of and Design Criteria for Deployable Aerodynamic Decelerators. Tech. Rep. No. ASD-TR-61-579, Air Force Flight Dynamics Lab., Wright-Patterson AFB, Dec. 1963.

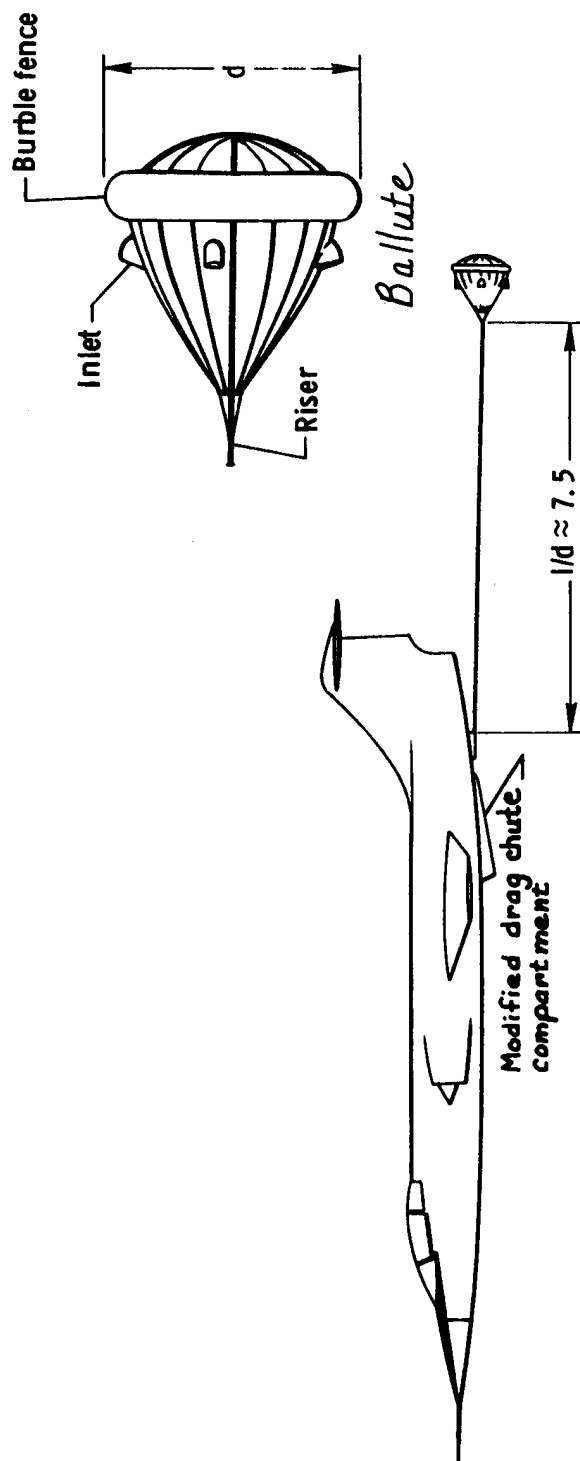
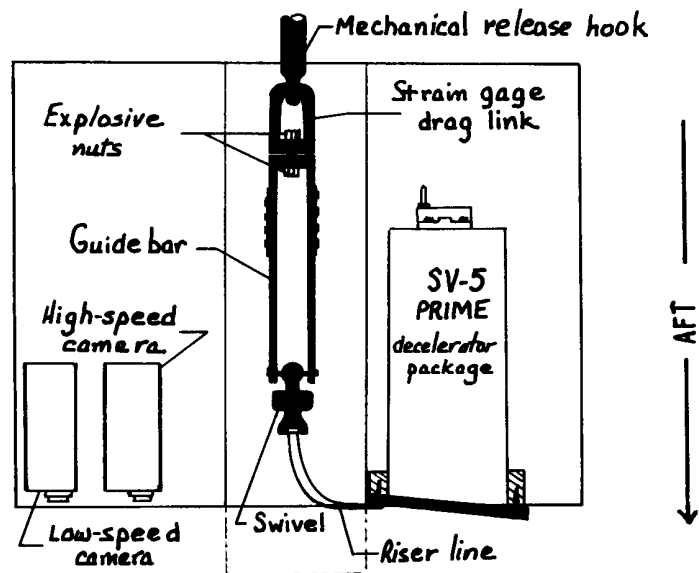
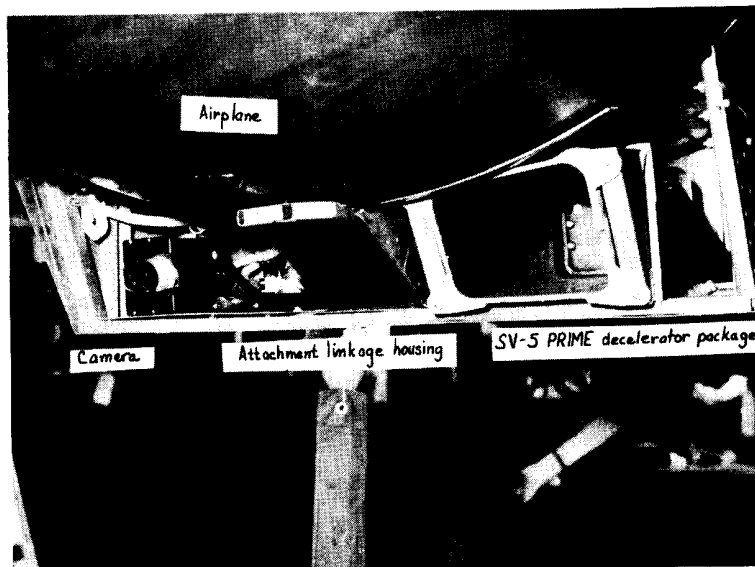


Figure 1. F-104B airplane towing a ballute decelerator.



(a) Planform drawing of the compartment.



(b) Aft view of the compartment.

Figure 2. Modification to the drag chute compartment of the airplane.

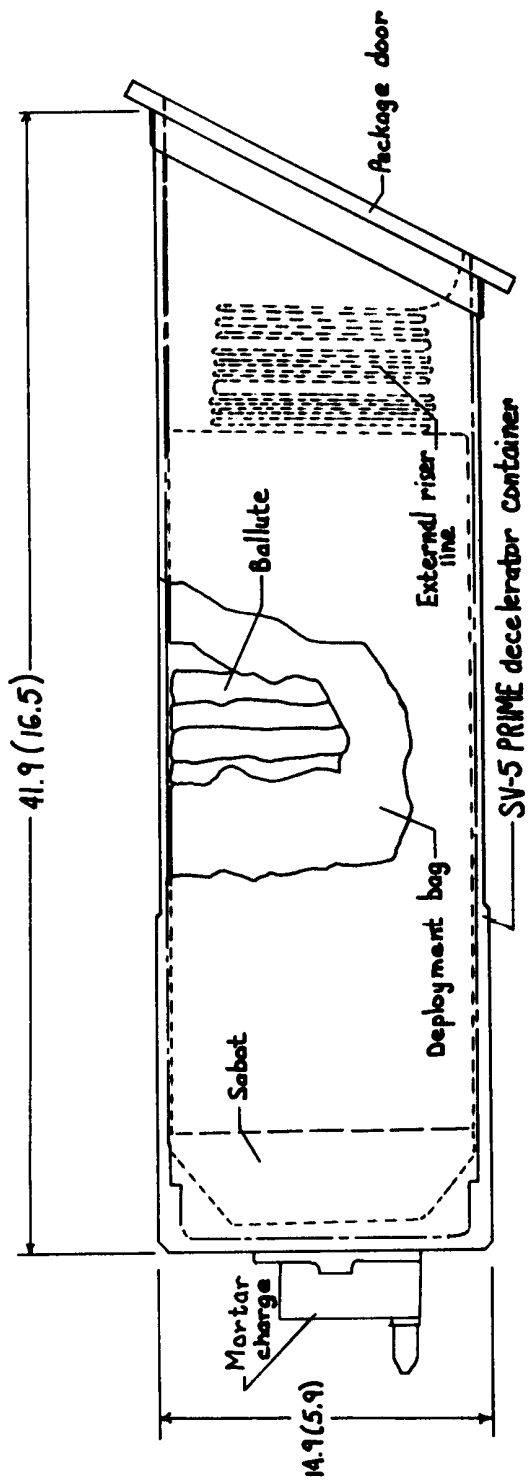
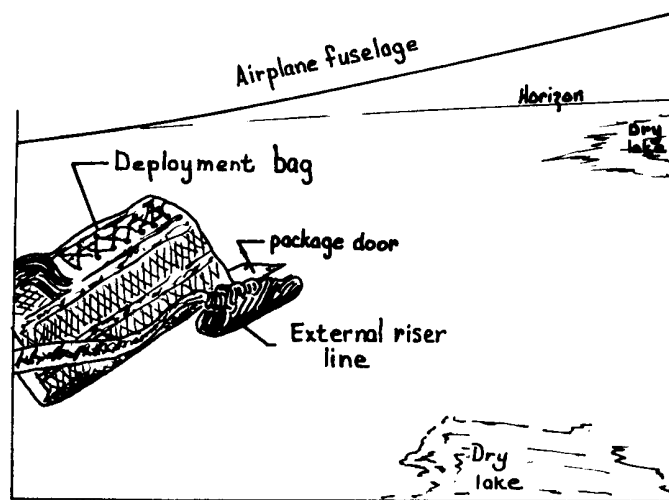
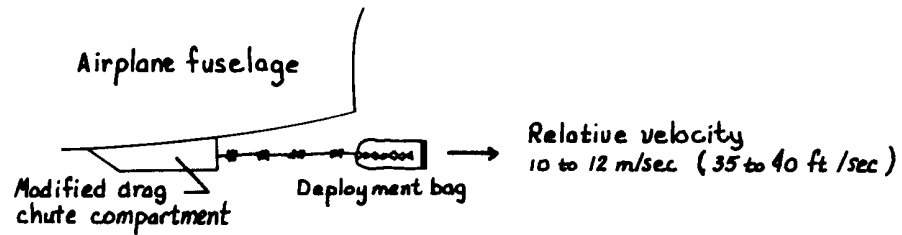


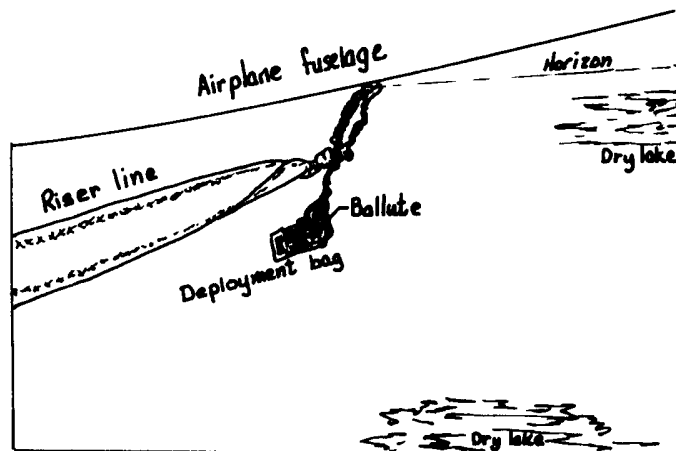
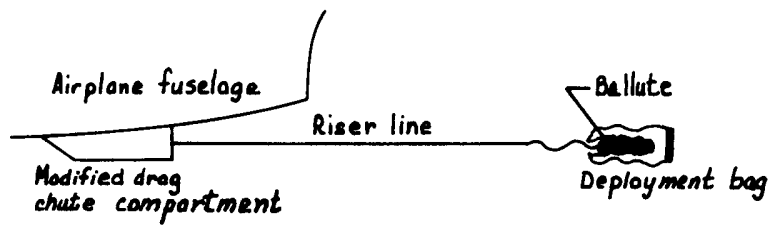
Figure 3. Cutaway view of the SV-5 PRIME decelerator package.

*Dimensions are in centimeters (inches).*



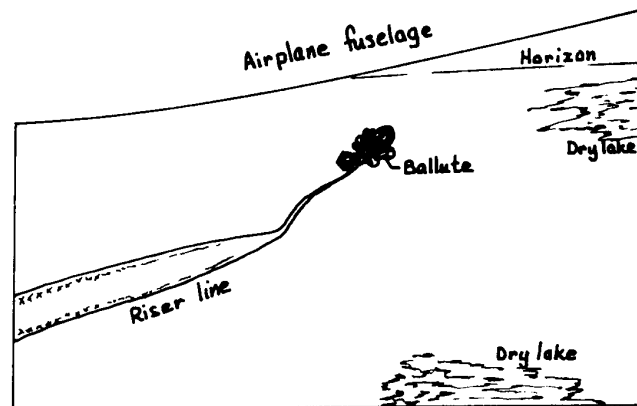
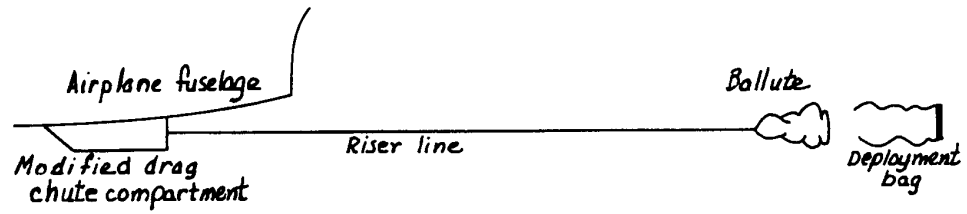
(a) Decelerator package just after firing mortar charge,  
 $t = 0.06 \text{ sec.}$

Figure 4. Deployment and inflation of the decelerator.



(b) Full extension of external riser line and release of ballute from deployment bag,  $t = 0.16$  sec.

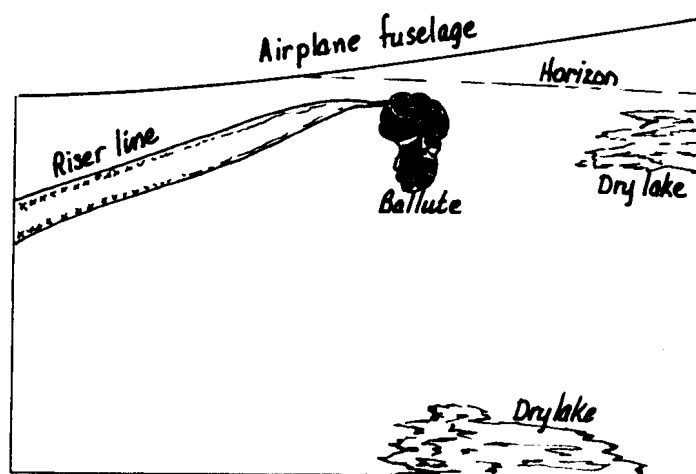
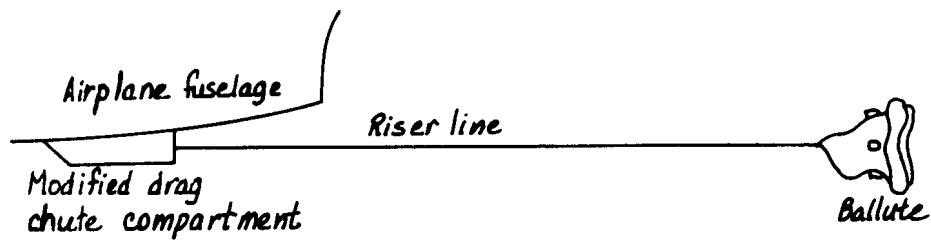
Figure 4 (continued).



(c) Separation of deployment bag from ballute  
at full riser line extension,  $t = 0.28$  sec.

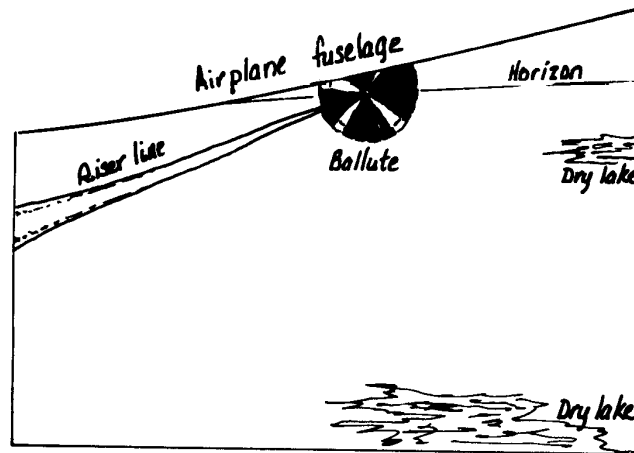
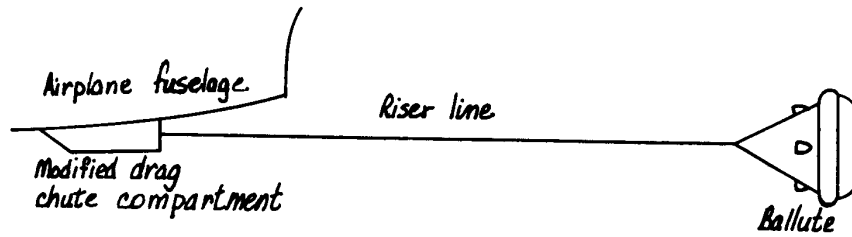
Figure 4 (continued).





(d) Beginning of ballute inflation,  $t = 0.35$  sec.

Figure 4 (continued).



(e) Ballute inflation completed,  $t = 1.0 \text{ sec.}$

Figure 4 (concluded).

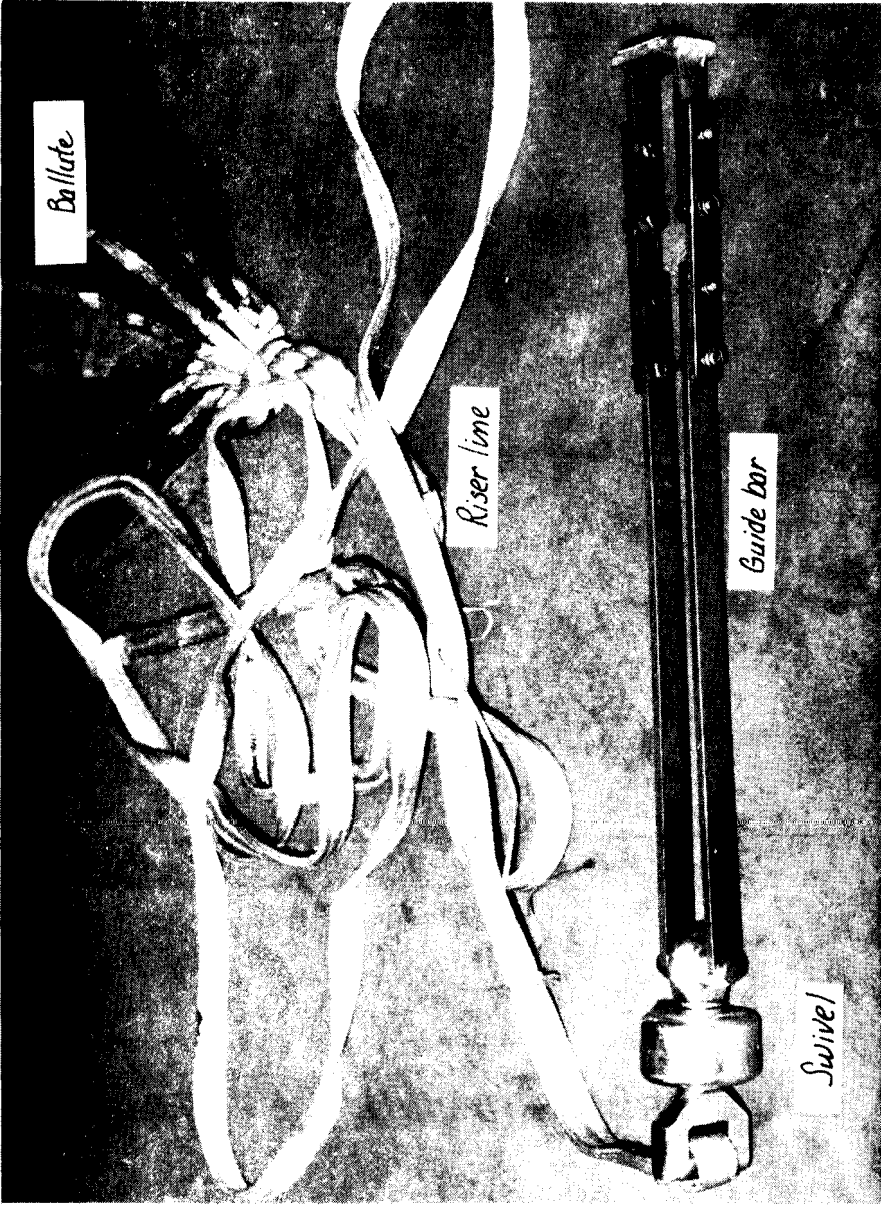
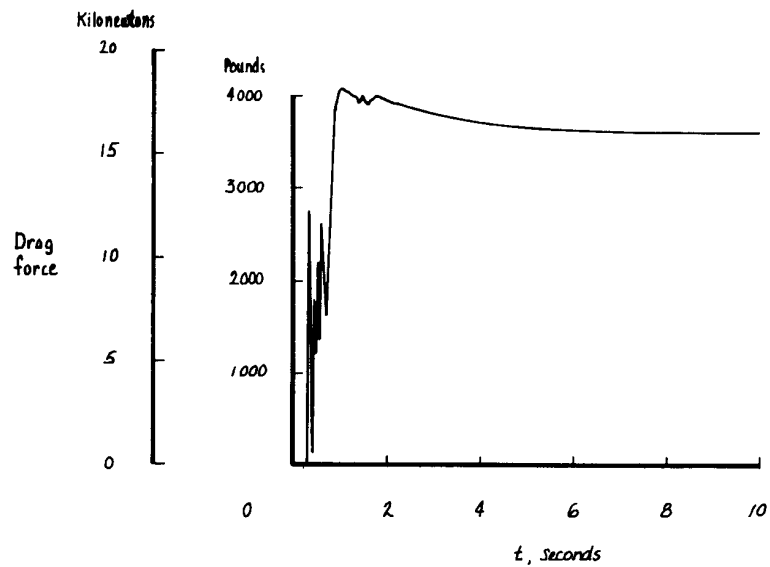
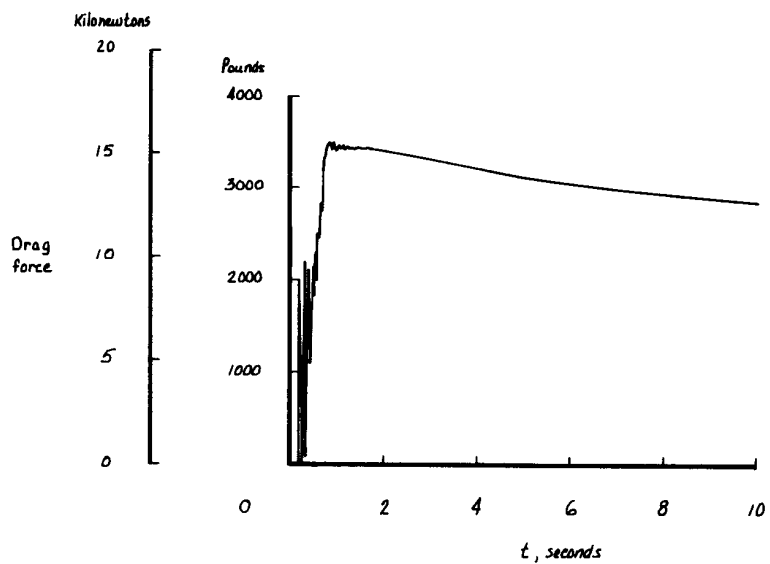


Figure 5. Modified attachment linkage from decelerator to drag link.

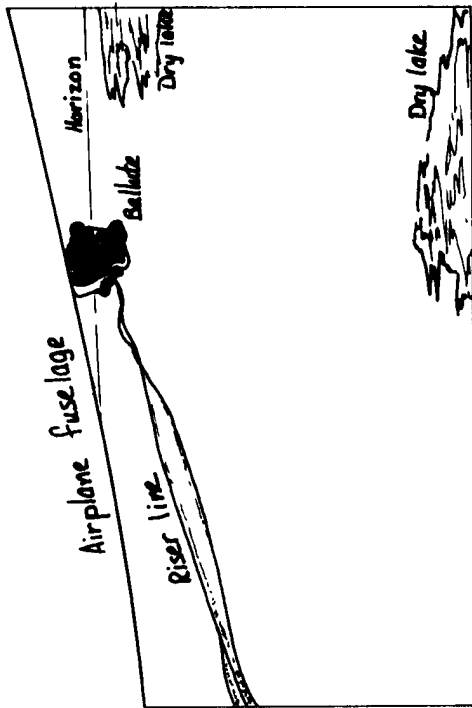


(a) Flight 1.

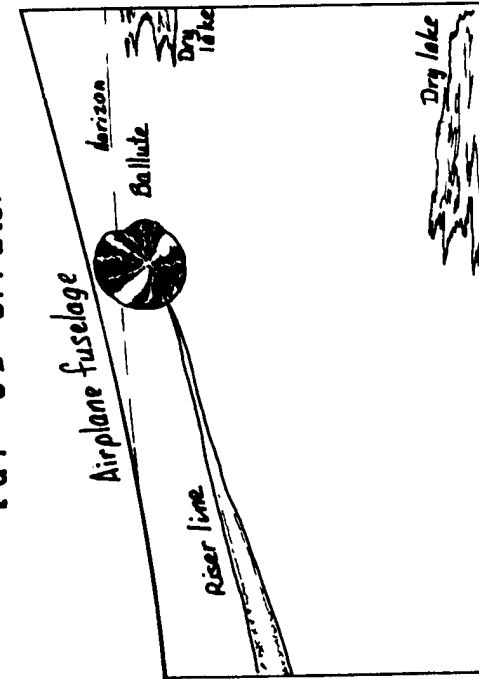


(b) Flight 2.

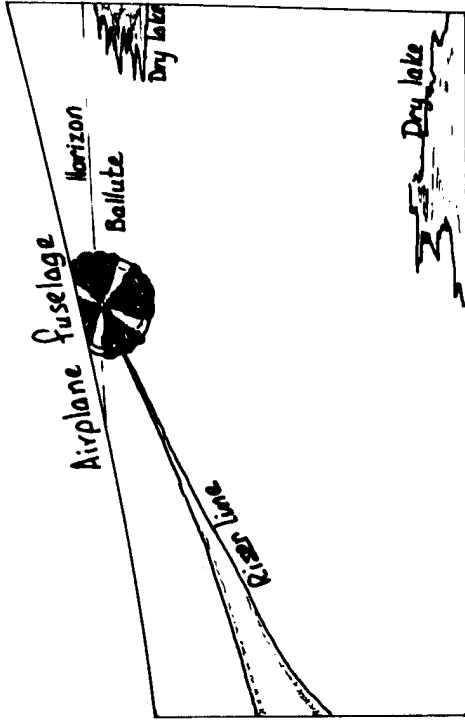
Figure 6. Time history of drag force during decelerator inflation.  $M = 1.3$  ;  $h = 15.25$  km (50,000 ft.).



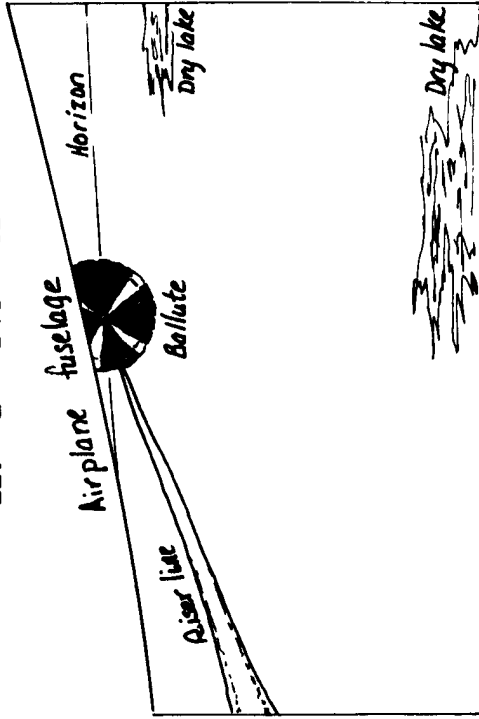
(a)  $t = 0.4 \text{ sec.}$



(b)  $t = 0.5 \text{ sec.}$

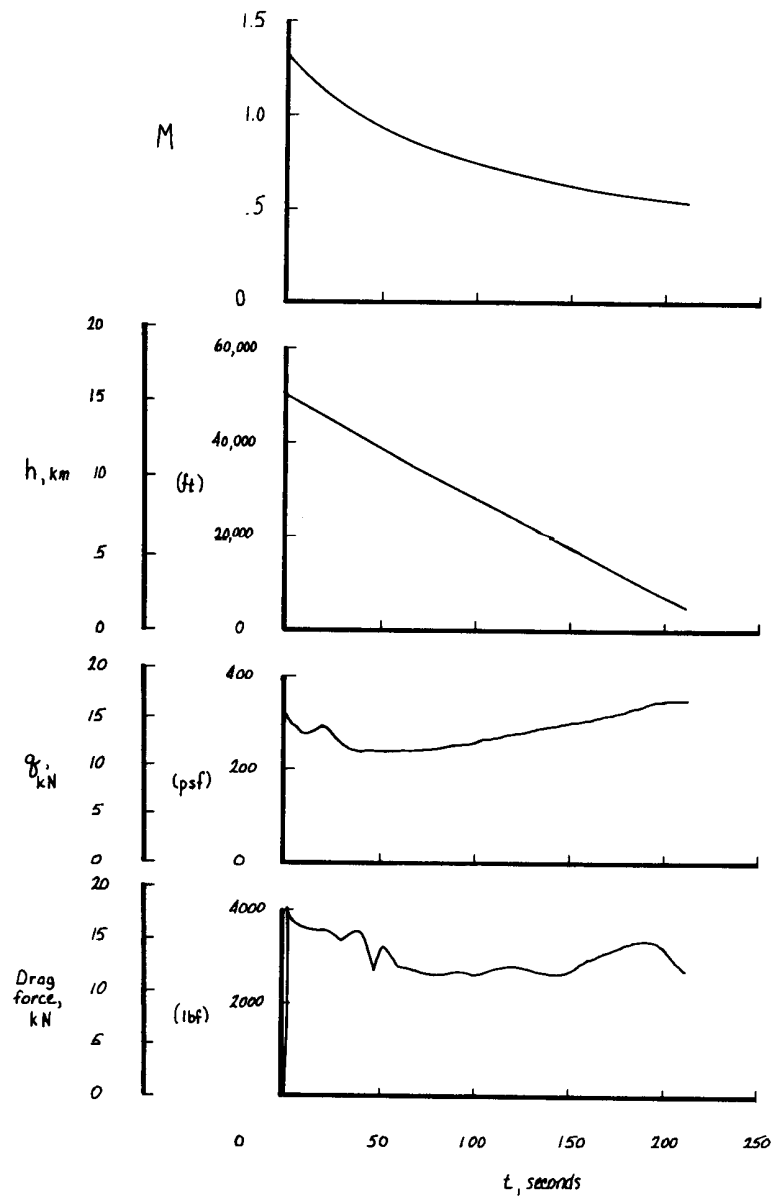


(c)  $t = 0.6 \text{ sec.}$



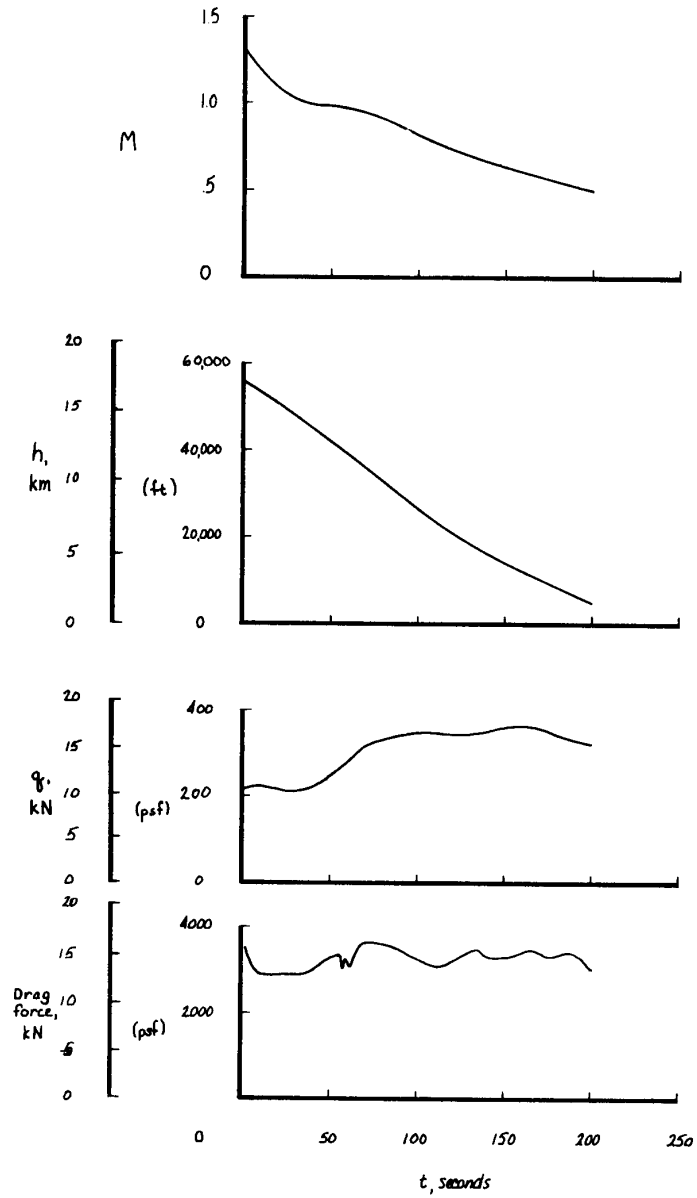
(d)  $t = 1.0 \text{ sec.}$

Figure 7. Inflation of decelerator as recorded with the high-speed camera.



(a) Flight 1.

Figure 8. Time history of deceleration.



(b) Flight 2.

Figure 8 (concluded).

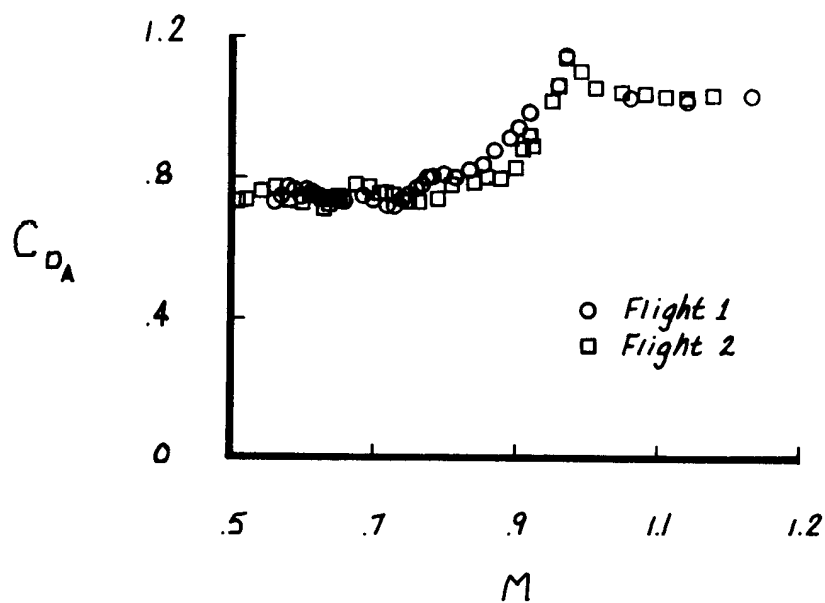


Figure 9. Drag coefficients for a ballute decelerator measured in flight.



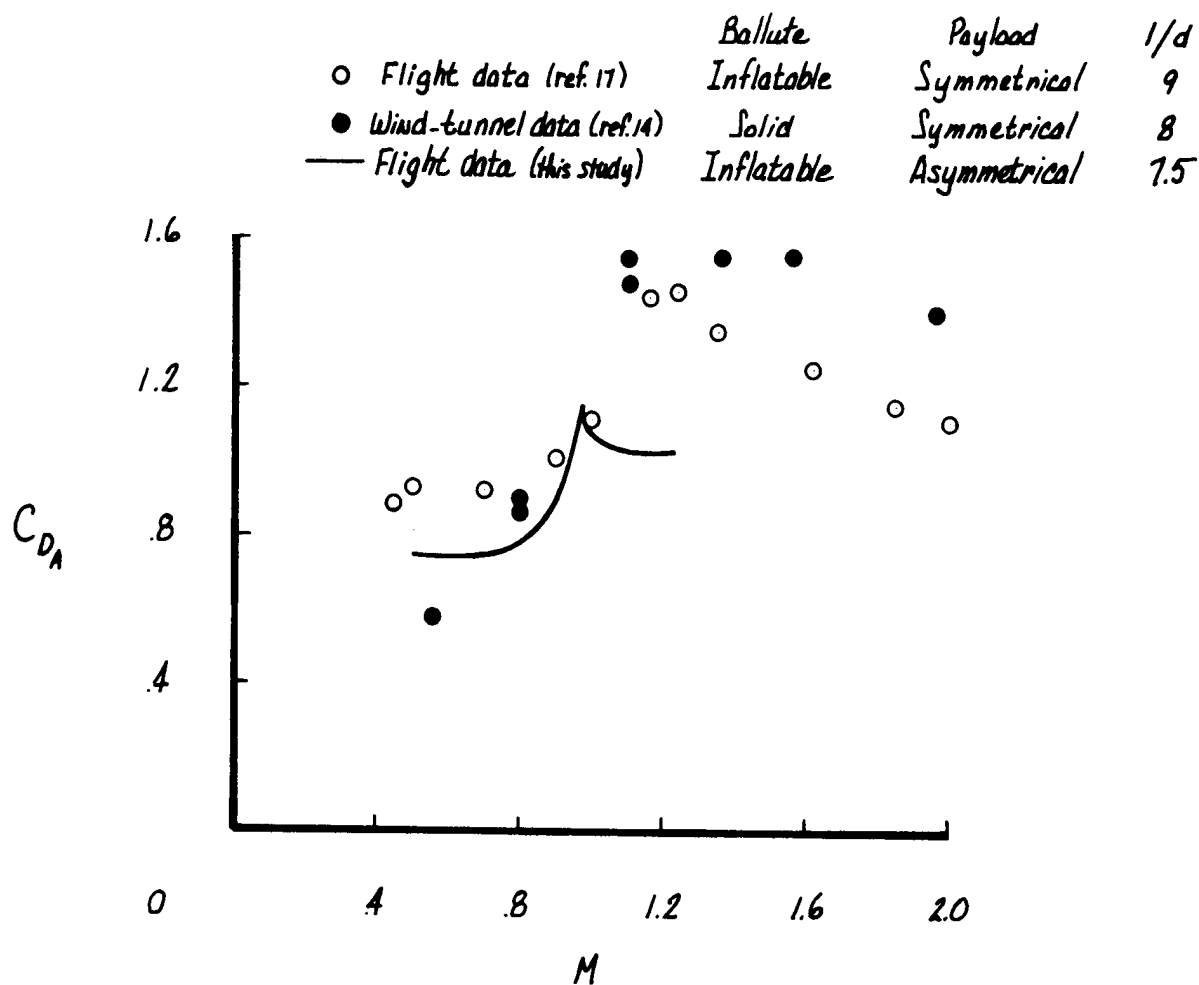
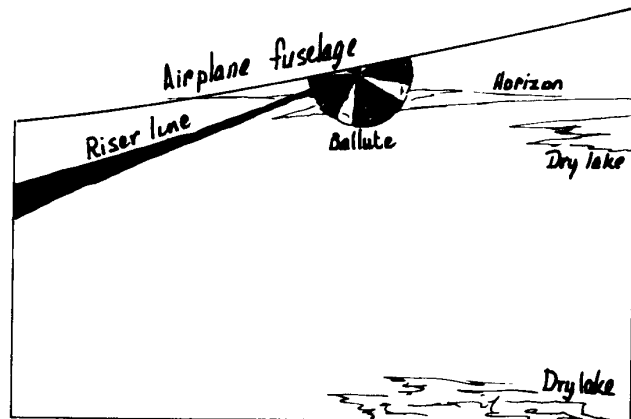
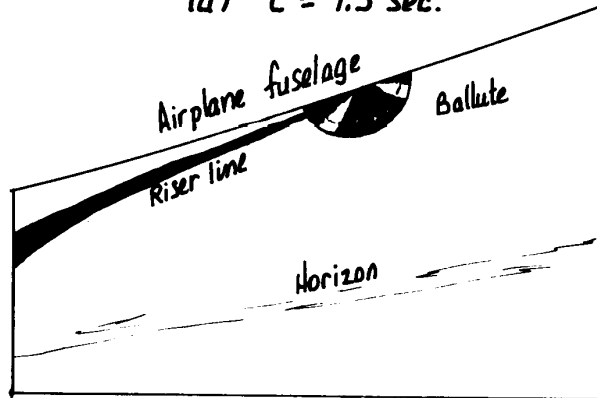


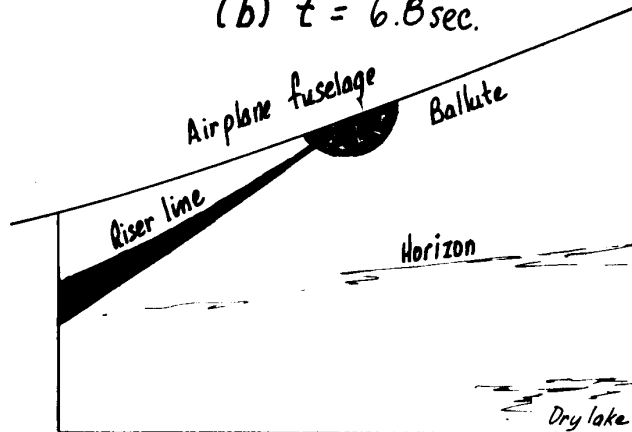
Figure 10. Comparison of ballute drag coefficients measured in flight and wind-tunnel tests for both symmetrical and asymmetrical bodies.



(a)  $t = 1.5 \text{ sec.}$



(b)  $t = 6.8 \text{ sec.}$



(c)  $t = 13.6 \text{ sec.}$

Figure 11. Location of decelerator in the wake of F-104B airplane at various times during typical deceleration.